Forestry Research

ARTICLE

Open Access

https://doi.org/10.48130/forres-0026-0035

Forestry Research **2026**, 6: e035

MuMYB116 confers salt tolerance in mulberry through a hormone-Ca^{2+} regulatory network

Chaorui Liu[1#], Teng Zhao[1#], Ming Sun[1], Gefan Wang[1], Shuo Lu[1], Leran Yv[1], Zhaoyang Liu[1], Yingping Gai[2*] and Xianling Ji[1*]

[1] *College of Forestry, Shandong Agricultural University, Taian, Shandong 271018, China*
[2] *College of Life Sciences, Shandong Agricultural University, Taian, Shandong 271018, China*
[#] Authors contributed equally: Chaorui Liu, Teng Zhao
[*] Correspondence: gyp@sdau.edu.cn (Gai Y); xlji@sdau.edu.cn (Ji X)

Abstract

Soil salt accumulation imposes major limitations on plant growth and long-term ecosystem stability. Mulberry exhibits moderate salt tolerance, but the molecular mechanisms of its salt-stress adaptation remain largely uncharacterized. Here, we functionally characterized MuMYB116, a salt-responsive, nuclear-localized R2R3-MYB transcription factor with conserved R2/R3 domains and an S20-subgroup-specific WxPRL motif. *MuMYB116* expression is induced by NaCl, abscisic acid (ABA), and methyl jasmonate (MeJA) but repressed by gibberellin (GA). Its role in salt tolerance was validated in heterologous *Arabidopsis* and in mulberry via hairy-root overexpression and VIGS-mediated gene silencing. *MuMYB116* overexpression promoted proline and flavonoid accumulation, reduced the accumulation of reactive oxygen species (ROS) and malondialdehyde (MDA), concomitant with increased antioxidant capacity. MuMYB116 functions as a key regulator coordinating plant growth and stress-defense responses, repressing development under non-stress conditions while activating protective responses under salt stress. Mechanistically, the upstream regulator MuBPC2 (a BBR-BPC family member) binds to and activates the *MuMYB116* promoter. MuMYB116 physically interacts with the calmodulin-like protein MuCML44, linking Ca^{2+} signaling to the salt-stress response. Moreover, MuMYB116 directly activates the flavonoid biosynthetic genes *MuFLS* (flavonol synthase) and *MuCHS* (chalcone synthase) by binding their promoters, explaining the elevated flavonoid abundance in the transgenic lines. Our findings reveal that MuMYB116 enhances salt tolerance through a multilayered network integrating hormone signaling, Ca^{2+} signal transduction, and physiological and metabolic responses. This work provides a useful molecular resource for developing salt-tolerant mulberry cultivars and a theoretical basis for the ecological restoration of saline soils.

Keywords: *Morus alba*; Salt tolerance; MYB transcription factor; Growth-defense trade-off; Calcium signaling; Flavonoid biosynthesis

Citation: Liu C, Zhao T, Sun M, Wang G, Lu S, et al. 2026. MuMYB116 confers salt tolerance in mulberry through a hormone-Ca^{2+} regulatory network. *Forestry Research* 6: e035 https://doi.org/10.48130/forres-0026-0035

Introduction

As a woody plant with prominent economic and ecological benefits, mulberry (*Morus alba* L.) plays an important role in agroforestry practices and ecological restoration initiatives[1,2]. Mulberry functions as the only dietary source for silkworms and represents a core resource that supports the long-term sustainable development of the sericulture industry. Moreover, mulberry roots, leaves, and fruit accumulate high levels of bioactive phytochemicals, particularly anthocyanins and flavonoids, which have considerable potential for applications in the nutraceutical and pharmaceutical industries[3–5]. Ecologically, mulberry has a well-developed root system that effectively anchors soil and mitigates erosion and sand encroachment, making mulberry an ideal species for windbreak and sand fixation in arid and semi-arid regions[6,7]. Mulberry also has considerable value for the bioremediation of saline soils[8,9]. Large-scale cultivation of mulberry in fragile ecosystems such as coastal saline soils and inland salinized areas can improve soil physicochemical properties, reduce soil salinity, restore vegetation cover, and safeguard regional ecological security.

Salinity stress in soils has emerged as a critical global challenge restricting the sustainable development of agriculture and forestry[10]. Soil salinity imposes adverse effects on more than 1 billion ha across the world, and the area of salinized soil continues to increase due to climate change and inappropriate agricultural practices[11]. High salinity inhibits plant growth through diverse physiological processes, mainly triggered by osmotic imbalance, harmful ion accumulation, and excessive reactive oxygen species (ROS)-mediated oxidative damage[12–14]. For mulberry, salt stress significantly inhibits seedling growth, suppresses photosynthetic efficiency, and causes leaf chlorosis, wilting, and even plant mortality[15,16]. Although mulberry has inherent salt tolerance, moderate to high salinity severely impairs its growth and ecological functions. This limits its wide application in saline soil remediation[17,18]. Therefore, breeding new mulberry varieties with enhanced salt tolerance is crucial to broaden its cultivation range, increase the utilization potential of saline soils, and enhance both economic and ecological benefits.

Plant stress-response processes are governed mainly by transcription factors, which fine-tune downstream gene expression by either activating or repressing transcription[19–23]. Transcription factors belonging to the MYB family form one of the largest transcription factor families in plants, and their members participate extensively in plant growth, developmental processes, secondary metabolic pathways, and responses to abiotic stresses[24–27]. Four subfamilies, including 1R, R2R3, 3R, and 4R, can be distinguished among MYB proteins by examining the conservation of their characteristic MYB domains[28–30]. Among these subgroups, R2R3-MYBs constitute the largest group and serve as key regulators in plant adaptation to salt stress[31–34]. For instance, AtMYB111 in *Arabidopsis* enhances salt tolerance through transcriptional activation of flavonoid biosynthetic genes[35]. In apple (*Malus pumila*), MdMYB108L improves salt

© The Author(s)

https://doi.org/10.48130/forres-0026-0035

tolerance by upregulating the vacuolar Na^+/H^+ antiporter gene *MdNHX1* and enhancing cellular ion compartmentalization[36]. In addition, some MYB transcription factors mediate phytohormone signaling cascades, such as ABA signaling, to coordinate plant stress responses[37–39]. Collectively, R2R3-MYB transcription factors serve as central regulatory components governing plant adaptation to salt stress and represent valuable targets for molecular breeding in woody species.

Advances in mulberry genomics have greatly accelerated research on MYB transcription factors. Genome-wide identification has uncovered 187 MYB-family members within the mulberry genome, but few have been functionally characterized, and their regulatory roles in salt-stress responses remain largely unexplored[40]. In our previous transcriptome profiling of salt-treated mulberry roots, we identified a strongly induced R2R3-MYB gene (*MuMYB116*), suggesting its potential role in the regulation of salt tolerance.

Here, we performed a comprehensive analysis of the genetic characteristics and expression dynamics of *MuMYB116*, verified its salt tolerance function in both heterologous and homologous systems, identified its upstream regulators and interacting proteins, and elucidated the molecular mechanisms by which it regulates salt tolerance in mulberry. Our findings establish a theoretical framework for understanding the regulatory network underlying salt tolerance in mulberry and provide genetic resources for breeding stress-resistant mulberry cultivars, facilitating the large-scale application of mulberry in saline-soil remediation and ecological restoration.

Materials and methods

Plant materials and culturing conditions

Morus atropurpurea cv. 'Guisang You 62' seedlings were cultured in a controlled-environment chamber maintained at 25 °C, under a 16-h light/8-h dark photoperiod and relative humidity of 60%–70%. Seedlings of *Arabidopsis thaliana* ecotype Col-0 and *Nicotiana benthamiana* were grown at a constant temperature of 22 °C under identical light and humidity settings. All *Arabidopsis* seeds were synchronized for uniform germination, transplanted on identical days, and randomly rotated in growth chambers to eliminate developmental heterogeneity before stress treatment.

Gene cloning and bioinformatics analysis

RNAiso reagent (TaKaRa) was employed to extract total RNA from mulberry leaf tissues, and PrimeScript RT Master Mix (TaKaRa) was used for first-strand cDNA synthesis. The full-length coding sequences (CDS) of *MuMYB116*, *MuBPC2* (a BBR-BPC family member), *MuCML44* (calmodulin-like protein CML44), *MuFLS* (flavonol synthase), and *MuCHS* (chalcone synthase) were amplified using primers designed specifically for each target gene. PCR amplicons were inserted into the TaKaRa-sourced pMD19-T cloning vector, and subsequent sequencing was performed to confirm correct insert sequences. DNAMAN V6 software was used for sequence alignment of MuMYB116 and its homologs retrieved from the NCBI database. A phylogenetic tree was constructed using the neighbor-joining (NJ) method in MEGA. Distance matrices were calculated based on the Poisson model, with 1,000 bootstrap replicates used to assess branch support.

Assessment of protein subcellular localization

The stop-codon-truncated *MuMYB116* coding sequence was fused to the green fluorescent protein gene (*GFP*) sequence in the pBI121 vector, yielding the recombinant plasmid 35S::MuMYB116-GFP. The empty vector 35S::GFP was used as a negative control, and co-infiltration was performed with 35S::NLS-mCherry, used as a nuclear marker. *Agrobacterium tumefaciens* GV3101 was transformed with the target plasmids, and the resulting bacterial suspensions were used for infiltration of *N. benthamiana* leaf tissues. After 3 d of incubation, GFP fluorescence signals were imaged using a Zeiss LSM880 laser-scanning confocal system (Carl Zeiss AG, Oberkochen, Germany), with excitation fixed at 488 nm and emission detection spanning 505–530 nm.

Quantitative real-time PCR (qRT-PCR) analysis

RNAiso reagent (TaKaRa) was used for total RNA extraction, and the PrimeScript RT Master Mix (TaKaRa) was used to produce first-strand cDNA. Amplification for qRT-PCR was conducted with ChamQ SYBR qPCR Master Mix (Vazyme, Nanjing, China) using the Bio-Rad CFX96 Real-Time PCR System (Bio-Rad, Hercules, USA). Two reference genes were used for each species to ensure accuracy: *AtActin* and *AtEF-1α* for *Arabidopsis*, and *MuActin* and *MuEF-1α* for mulberry. Relative transcript abundances were determined by the $2^{-\Delta\Delta C_T}$ method[41], with normalization to the geometric mean of the two reference genes. Each assay included three biological replicates and three technical replicates.

Plant transformation

For stable transformation of *Arabidopsis*, the gene of interest was first subcloned into the pLGNL binary vector, which was then mobilized into *A. tumefaciens* GV3101, and floral dipping was applied to achieve plant transformation. Transformed seedlings were first selected on kanamycin-containing MS medium, after which stable transgenic lines were verified using genomic PCR together with qRT-PCR assays. Three independent homozygous overexpressing lines exhibiting high transcript levels were chosen for follow-up experiments.

To generate transgenic mulberry hairy roots, the target coding sequence was inserted into the pBI121 vector, and the resulting construct was introduced into *Agrobacterium rhizogenes* K599. Mulberry hypocotyls were infected with *A. rhizogenes* K599 cultures, and transgenic hairy roots were induced on MS medium. Positive transgenic hairy roots were identified by qRT-PCR and genomic PCR.

To perform VIGS-mediated gene silencing, a 300-bp coding-sequence fragment of *MuMYB116* was inserted into the pTRV2 vector. Both the recombinant pTRV2-MuMYB116 and empty pTRV2 (control) were then separately delivered into *A. rhizogenes* K599 and used to generate MuMYB116-silenced hairy roots in mulberry.

For transient transformation in mulberry leaves, the third fully expanded young leaves were collected from the 'Guisang You 62' seedlings at 5 weeks of age and immersed in an *Agrobacterium* suspension. Vacuum infiltration was applied three times at 5 min per cycle to facilitate *Agrobacterium* infection. Upon completion of infiltration treatment, absorbent cotton was used to wrap the leaf petioles. The treated leaves were then incubated in Petri dishes for 2 d before downstream analysis.

Plant treatment

To perform seed germination tests, wild-type and transgenic seeds were first surface-sterilized, then plated on 1/2 MS solid

medium supplemented with 0 or 100 mmol·L^{-1} NaCl. Seed germination rates were recorded daily for 7 d. To quantify primary root elongation, seeds were vertically cultured on identical medium, and root lengths were measured at 7 d post-germination. For soil-based salt-stress experiments, 4-week-old uniformly sized *Arabidopsis* seedlings were irrigated with NaCl solution at concentrations of 200 or 300 mmol·L^{-1}. Plant morphological phenotypes and survival rates were documented after stress treatment. For mulberry leaf disc salt treatment, transiently transformed mulberry leaves were punched into 1.5-cm-diameter leaf discs. For phenotypic characterization, the prepared leaf discs were arranged on filter-paper-lined Petri dishes moistened with 0 or 300 mmol·L^{-1} NaCl solution.

To conduct exogenous hormone assays, mulberry seedlings at the 4-week growth stage were sprayed with 50 μmol·L^{-1} ABA, 100 μmol·L^{-1} methyl jasmonate (MeJA), or 100 μmol·L^{-1} gibberellin (GA). At time points of 2, 4, 6, and 8 h after treatment, leaf samples were excised, promptly quenched in liquid nitrogen, and subsequently preserved at −80 °C until processing.

For Ca^{2+} inhibitor treatment, 4-week-old wild-type *Arabidopsis* and *MuMYB116*-overexpressing transgenic seedlings were pretreated with 10 mmol·L^{-1} $LaCl_3$ (a Ca^{2+} channel inhibitor) for 24 h, followed by irrigation with NaCl solution at a concentration of 200 mmol·L^{-1}. Plant phenotypes were photographed, and survival rates were recorded after treatment. All treatment concentrations were selected according to previously validated protocols for mulberry and *Arabidopsis*[42,43], which reliably induce reproducible stress phenotypes and gene expression responses.

GUS histochemical staining assay

To produce the pMuMYB116::GUS reporter construct, the *MuMYB116* promoter fragment was isolated by PCR from mulberry genomic DNA and inserted into the pBI121 vector. After transformation of the recombinant plasmid into *A. tumefaciens* GV3101, the resulting bacterial suspension was used for infiltration of *N. benthamiana* leaves. After 3 d of incubation, the tissues were immersed in GUS staining solution and vacuum-infiltrated for 15–20 min. After 12 h of incubation at 37 °C in complete darkness, the samples were repeatedly bleached in 70% ethanol to remove chlorophyll and were then imaged using a stereomicroscope.

Yeast one-hybrid (Y1H) assays

To produce the prey plasmid pGADT7-MuBPC2, the *MuBPC2* coding sequence was ligated into the pGADT7 vector (Clontech, Mountain View, USA). For bait vector construction, the amplified *MuMYB116* promoter fragment (pMuMYB116) was subcloned into pAbAi, producing the recombinant bait plasmid pAbAi-pMuMYB116. Following linearization, the bait plasmid was integrated into the genome of yeast Y1HGold. The prey construct, or empty pGADT7 vector (negative control), was subsequently transformed into the bait strain. For assessment of protein-DNA binding activity, transformants were cultured on SD/-Leu medium supplemented with the selective agent Aureobasidin A (AbA) and incubated at 30 °C for 3–5 d.

Electrophoretic mobility shift assay (EMSA)

GST-MuBPC2 fusion protein and GST alone (negative control) were heterologously produced in *Escherichia coli*, followed by protein purification with glutathione-Sepharose affinity resin. Purified recombinant proteins were incubated with a biotin-tagged probe carrying the MuBPC2 recognition motif within the *MuMYB116* promoter region. In competitive binding experiments, an unlabeled competitor probe was added at a 100-fold molar excess. Complex formation was monitored by native gel electrophoresis, followed by chemiluminescent detection according to the manufacturer's protocol (Thermo Fisher Scientific).

Dual-luciferase reporter assay

For the MuBPC2-MuMYB116 interaction, the *MuBPC2* CDS was recombined into the pGreenII 62-SK plasmid to construct the 35S::MuBPC2 effector. Meanwhile, pMuMYB116 was ligated into pGreenII 0800-LUC to produce the pMuMYB116::LUC reporter. For the negative control, the empty pGreenII 62-SK was co-infiltrated with pMuMYB116::LUC.

For the MuMYB116-downstream target assay, the CDS of *MuMYB116* was inserted into the pGreenII 62-SK vector for effector construct generation. Promoter regions of *MuFLS* and *MuCHS* were separately recombined into pGreenII 0800-LUC to yield the corresponding reporter plasmids.

Agrobacterium strains carrying the effector or reporter constructs were mixed and co-infiltrated into *N. benthamiana* leaves. After 3 d of incubation, leaf luciferase signals were imaged on a Tanon 5200 multifunctional imaging system (Tanon, Shanghai, China) after applying luciferase substrate (Promega, Madison, USA).

Yeast two-hybrid (Y2H) assay

To generate the prey and bait constructs, the CDSs of *MuMYB116* and *MuCML44* were individually inserted into the pGADT7 (prey) and pGBKT7 (bait) vectors, respectively. The bait and prey vectors were co-introduced into Y2HGold-competent yeast cells. The resulting transformants were spread onto DDO (SD/-T/-L), QDO (SD/-T/-L/-A/-H), and X-α-gal-amended QDO plates. All plates were incubated in an inverted position at 28 °C for approximately 1 week to observe colony growth.

Luciferase complementation assay (LCI)

To generate split-luciferase reporter constructs, the *MuMYB116* CDS was inserted upstream of the N-terminal luciferase moiety (NLuc) in the pCAMBIA1300-NLuc vector. Meanwhile, the coding region of *MuCML44* was ligated to the C-terminal luciferase segment (CLuc) using the pCAMBIA1300-CLuc vector. The recombinant plasmids were introduced into *A. tumefaciens* strain GV3101, followed by agroinfiltration into leaf tissues of *N. benthamiana*. The combinations of NLuc-MuMYB116 + CLuc and NLuc + CLuc-MuCML44 were used as negative controls. After 48 h of incubation, luciferase substrate was sprayed onto the leaves, and luminescence signals were captured on a Tanon 5200 multifunctional imager (Tanon).

Pull-down assay

GST-MuMYB116 and GST alone (negative control) were heterologously expressed in *E. coli* BL21, followed by purification with glutathione-Sepharose 4B affinity resin. Recombinant His-tagged MuCML44 was produced and purified using agarose resin. Purified His-MuCML44 was then co-incubated with GST or GST-MuMYB116 pre-immobilized on glutathione-Sepharose beads in binding buffer at 4 °C for 4 h. Upon completion of five sequential washing cycles, captured proteins were eluted. The resulting samples were resolved by SDS-PAGE before being analyzed by western blotting with anti-His and anti-GST antibodies. Input samples (10%) were included as loading controls.

https://doi.org/10.48130/forres-0026-0035

Biochemical measurements

ROS accumulation was visualized in planta by histochemical staining. H_2O_2 accumulation was detected using 3,3'-diaminobenzidine (DAB) staining. For O_2^- detection, nitroblue tetrazolium (NBT) staining was used. The Plant Tissue ROS Detection Kit (Solarbio, Beijing, China) was utilized for both assays according to the manufacturer's instructions. Proline and malondialdehyde (MDA) contents were quantified using detection kits (Solarbio, Beijing, China). A modified aluminum-nitrate colorimetric assay was used to determine total flavonoid content[44]. Spectrophotometric measurement of chlorophyll was performed as reported in a prior study[45].

Statistical analysis

All experiments included at least three independent biological replicates and three technical replicates, with results reported as mean ± SD ($n \geq 3$ biological replicates). SPSS 26.0 software (IBM, Armonk, USA) was utilized for statistical analysis. Comparisons between two experimental groups were performed using Student's *t*-test, where * $p < 0.05$ and ** $p < 0.01$ were considered statistically significant. Comparisons among multiple groups were assessed using one-way ANOVA. Post hoc pairwise comparisons were performed using Tukey's HSD test ($p < 0.05$). Different lowercase letters indicate significant differences.

Results

Identification and characteristics of *MuMYB116*

Transcriptome profiling of salt-treated mulberry roots identified 37 differentially expressed *MYB* genes, among which L484_015440 showed the most significant upregulation (Fig. 1a). Sequence alignment confirmed that L484_015440 is an ortholog of *Arabidopsis* MYB116 and contains two conserved R2/R3 MYB domains as well as the S20-subgroup-specific WxPRL motif (Fig. 1b). Phylogenetic analysis confirmed that this gene, designated *MuMYB116*, clusters with the *Arabidopsis* R2R3-MYB S20 subgroup (Fig. 1c). Subcellular localization analysis revealed that the 35S::MuMYB116-GFP fusion protein exhibited exclusive nuclear signals and overlapped with the mCherry-NLS nuclear marker, while the empty 35S::GFP control was distributed throughout the cell (Fig. 1d). This observation supports its putative role as a transcription factor.

Tissue and stress-induced expression patterns of *MuMYB116*

qRT-PCR analysis revealed that *MuMYB116* transcripts could be detected in every tissue sampled. Transcript abundance was highest in roots, intermediate in leaves, and lowest in stems (Fig. 2a). We next characterized the dynamic transcriptional responses of *MuMYB116* to hormone and salt treatments. qRT-PCR results indicated that *MuMYB116* transcript levels were significantly induced by

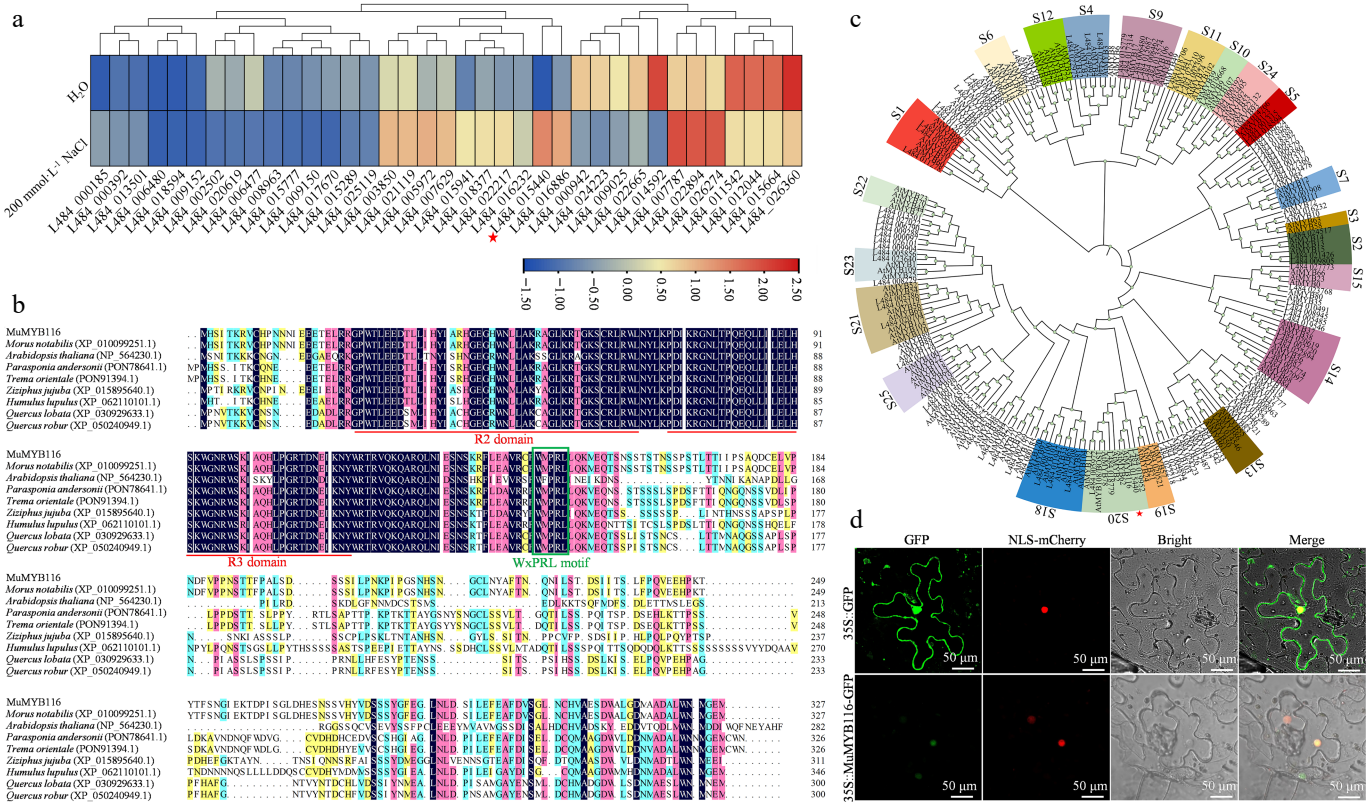


Fig. 1 Identification and phylogenetic analysis of MuMYB116 in mulberry. (a) Heatmap of differentially expressed MYB genes in salt-treated mulberry roots based on transcriptome data ($\log_2$fold change > 1 or < −1, $p < 0.05$). Locus L484_015440 (annotated as *MuMYB116*) is marked with a red asterisk. (b) Multiple sequence alignment showing conserved R2 and R3 MYB domains and the S20 subgroup-specific WxPRL motif of MuMYB116 and homologous proteins. (c) Neighbor-joining phylogenetic tree of R2R3-MYB proteins from *Arabidopsis* and *Morus notabilis* constructed with 1,000 bootstrap replicates. MuMYB116 (marked with a red asterisk) clusters within the *Arabidopsis* S20 subgroup. (d) Subcellular localization of 35S::MuMYB116-GFP in *Nicotiana benthamiana* leaf epidermal cells. 35S::NLS-mCherry serves as the nuclear marker, and empty 35S::GFP is the negative control. Scale bar as indicated.

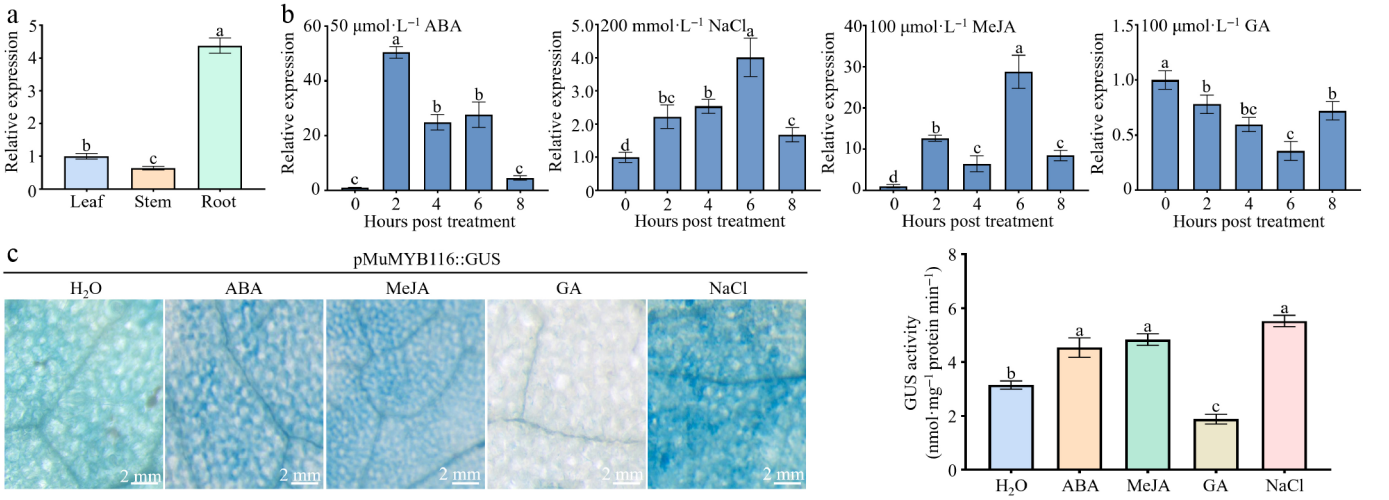


Fig. 2 Tissue- and stress-induced expression profiles of *MuMYB116* and its promoter activity. (a) Tissue-specific expression of *MuMYB116* in mulberry. (b) Dynamic transcriptional changes of *MuMYB116* under hormone and salt treatments. Four-week-old mulberry seedlings were treated with 100 μmol·L^{-1} MeJA, 100 μmol·L^{-1} GA, 50 μmol·L^{-1} ABA, or 200 mmol·L^{-1} NaCl. (c) GUS histochemical staining and activity assay of the *MuMYB116* promoter (pMuMYB116) in transiently transformed tobacco leaves under different treatments. Blue coloration indicates GUS activity driven by pMuMYB116. Data are presented as mean ± SD (n = 3 biological replicates). Different lowercase letters indicate significant differences (one-way ANOVA with Tukey's HSD test, $p < 0.05$).

ABA, MeJA, and NaCl, but markedly repressed by GA. Specifically, *MuMYB116* expression peaked at 6 h under both MeJA and NaCl treatments. In contrast, its expression was sharply upregulated at 2 h following ABA treatment, and then progressively declined toward basal levels by 8 h. Meanwhile, GA treatment suppressed *MuMYB116* expression, with the lowest level detected at 6 h (Fig. 2b).

To further explore these expression patterns, we cloned the promoter region of *MuMYB116* (pMuMYB116) and generated pMuMYB116::GUS reporter constructs for transient tobacco expression. Both GUS histochemical staining assays and quantitative activity measurements indicated that pMuMYB116 activity was significantly induced by ABA, MeJA, and NaCl, while GA treatment significantly reduced its activity (Fig. 2c). These findings demonstrated that the transcriptional response of *MuMYB116* to these treatments is consistent with the regulatory activity of its promoter.

MuMYB116 regulates plant growth and flowering under normal conditions

For functional characterization of *MuMYB116* within a heterologous system, stable *MuMYB116*-overexpressing (OE) *Arabidopsis* lines were constructed. Genomic PCR validated the integration of the *MuMYB116* transgene in the generated transgenic lines (Supplementary Fig. S1a), and qRT-PCR confirmed significantly elevated *MuMYB116* transcript levels in all OE lines compared with wild-type (WT) plants (Supplementary Fig. S1b). Phenotypic observations under non-stress conditions revealed that OE lines displayed substantially shorter primary roots relative to WT plants at 7 d post-germination (Fig. 3a). At 2–3 weeks after germination, OE plants displayed severe dwarfism with fewer and smaller rosette leaves compared to WT plants. However, this growth difference gradually disappeared at the 4-week stage, with no significant differences in leaf number and size between OE and WT plants (Fig. 3b, c). Notably, transgenic lines showed pronounced delays in bolting and flowering compared to WT plants (Fig. 3d). Molecular detection of flowering regulatory genes showed that *MuMYB116* overexpression significantly upregulated the flowering-repressor gene *AtFLC* and downregulated the flowering promoter gene *AtFT* (Fig. 3e). Collectively, these observations suggest that *MuMYB116* overexpression represses both vegetative and reproductive growth in *Arabidopsis* under normal growth conditions.

MuMYB116 confers salt tolerance in transgenic *Arabidopsis*

We first performed salt-stress phenotypic assays in heterologous *Arabidopsis* to assess whether *MuMYB116* enhances salt tolerance. Under 100 mmol·L^{-1} NaCl treatment, seeds of OE lines exhibited significantly higher germination rates than WT seeds over a 7-d observation period (Fig. 4a). Moreover, under 200 mmol·L^{-1} NaCl treatment, fully synchronized 4-week-old OE plants exhibited milder leaf chlorosis and wilting symptoms than WT plants and maintained a significantly higher survival rate (Fig. 4b).

Physiological parameter measurements indicated that OE plants accumulated higher levels of proline (Fig. 4c) and flavonoids (Fig. 4d), and lower MDA content (Fig. 4e) than WT plants under salt stress. In addition, OE plants showed reduced accumulation of ROS, as evidenced by lighter NBT and DAB staining, indicating lower O_2^- and H_2O_2 accumulation, respectively (Fig. 4f, g). These findings demonstrated that overexpression of *MuMYB116* confers improved salt-stress tolerance in transgenic *Arabidopsis* by regulating multiple physiological and metabolic pathways. Combined with the growth-suppressive phenotype under non-stress conditions, these results reveal a conserved growth-defense trade-off mediated by *MuMYB116*. It restricts plant growth under optimal conditions to allocate metabolic resources toward stress defense, which confers robust salt resistance under salt stress.

MuMYB116 directly activates flavonoid biosynthetic genes *MuFLS* and *MuCHS*

The elevated flavonoid abundance in salt-stressed OE plants prompted us to test whether MuMYB116 directly activates the

https://doi.org/10.48130/forres-0026-0035

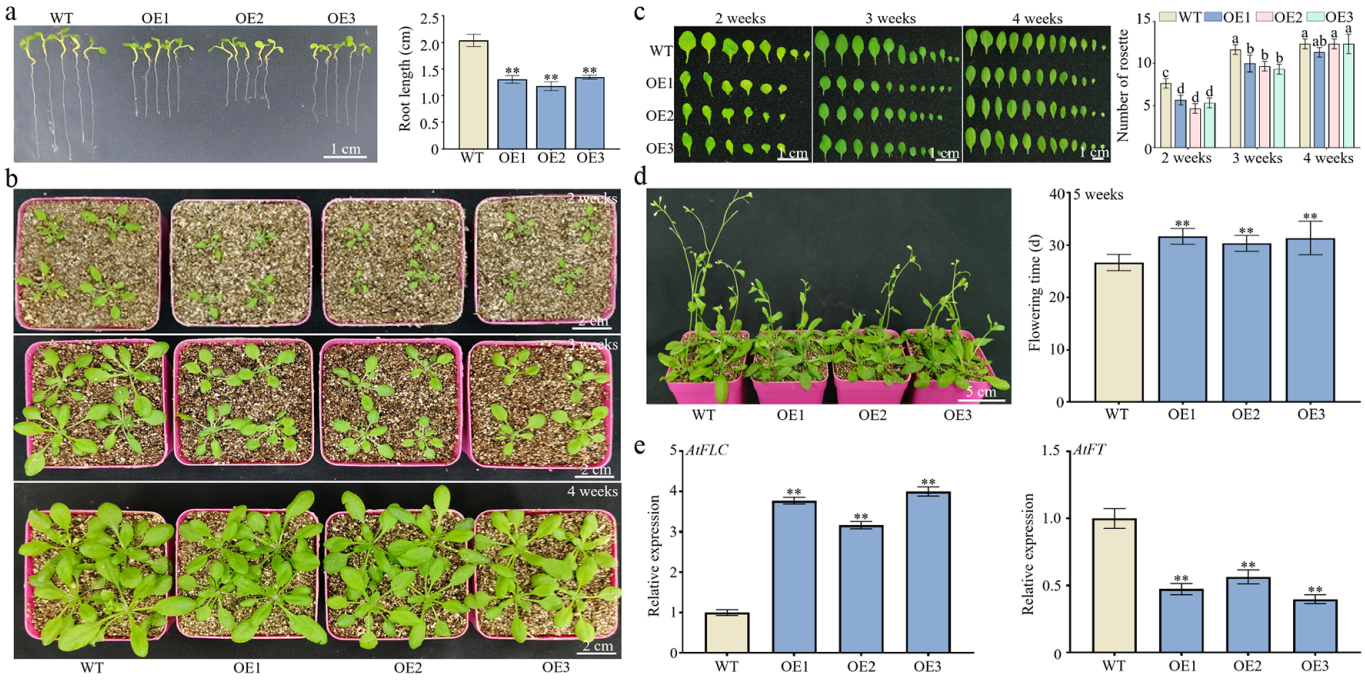


Fig. 3 Developmental phenotypes of *MuMYB116*-overexpressing and wild-type *Arabidopsis* under normal growth conditions. (a) Primary root lengths between 7-d-old wild-type (WT) and *MuMYB116*-overexpressing (OE) seedlings grown on 1/2 MS medium. Data are presented as mean ± SD (n = 15 biological replicates); ** $p < 0.01$ (Student's t-test). (b) Phenotypes of synchronized 2–4-week-old WT and OE *Arabidopsis* plants/seedlings. (c) Statistical quantification of rosette leaf number at 2, 3, and 4 weeks. Data are presented as mean ± SD (n = 15 biological replicates). Different lowercase letters indicate significant differences (one-way ANOVA with Tukey's HSD test, $p < 0.05$). (d) Bolting and flowering phenotypes of 5-week-old plants with quantified flowering time. Data are presented as mean ± SD (n = 15 biological replicates); ** $p < 0.01$ (Student's t-test). (e) Expression levels of *AtFLC* and *AtFT* genes. Data are presented as mean ± SD (n = 3 biological replicates); ** $p < 0.01$ (Student's t-test).

transcription of flavonoid biosynthetic genes. Bioinformatic analysis using PlantCARE identified conserved MYBCORE motifs within the promoter fragments of *MuFLS* and *MuCHS*. Dual-luciferase reporter experiments showed that co-transformation with 35S::MuMYB116 substantially elevated the LUC-to-REN activity ratio of pMuFLS::LUC and pMuCHS::LUC reporters relative to empty effector controls (Fig. 5a). EMSA assays showed that purified His-MuMYB116 specifically bound biotin-labeled MYBCORE motifs from *MuFLS* and *MuCHS* promoters, and excess unlabeled competitor probes abolished the shifted bands (Fig. 5b). These results demonstrate that MuMYB116 directly binds to and activates the promoters of *MuFLS* and *MuCHS*, providing a mechanistic basis for the enhanced flavonoid accumulation under salt stress.

Salt-tolerant function of *MuMYB116* in mulberry

To validate the salt tolerance function of *MuMYB116* in its native host, we employed an *Agrobacterium*-mediated mulberry hairy root transformation system. Genomic PCR analysis confirmed the integration of the *MuMYB116* transgene in the transgenic hairy roots (Supplementary Fig. S2a). GUS staining and qRT-PCR assays verified robust *MuMYB116* overexpression in the generated transgenic hairy roots (Fig. 6a). Under 300 mmol·L^{-1} NaCl treatment, mulberry seedlings harbouring *MuMYB116*-overexpressing hairy roots displayed milder leaf curling and wilting symptoms (Fig. 6b), accompanied by significantly higher survival rates relative to empty-vector control seedlings (Fig. 6c). Physiological analysis showed that under salt stress, mulberry seedlings with *MuMYB116*-overexpressing hairy roots accumulated higher levels of proline and flavonoids but lower levels of MDA compared to controls (Fig. 6d). These results from the mulberry hairy root system confirm that *MuMYB116* enhances salt tolerance in its native host, corroborating and extending the observations derived from transgenic *Arabidopsis*.

To confirm that *MuMYB116* is required for salt tolerance in mulberry, we performed a loss-of-function experiment using VIGS. Genomic PCR analysis verified the successful infection and integration of the pTRV2-MuMYB116 construct in the silenced hairy roots (Supplementary Fig. S2b). qRT-PCR data indicated that *MuMYB116* transcript abundance was substantially reduced in pTRV2-MuMYB116 seedlings compared to pTRV2-00 controls (Fig. 7a), confirming effective gene silencing. Under 300 mmol·L^{-1} NaCl stress, pTRV2-MuMYB116 seedlings exhibited more severe leaf chlorosis and wilting than pTRV2-00 controls (Fig. 7b), resulting in a significantly lower survival rate (Fig. 7c). Physiological measurements revealed that silenced seedlings maintained lower proline (Fig. 7d) and flavonoid contents (Fig. 7e) and higher MDA content (Fig. 7f) compared to the controls, indicating increased oxidative damage under salt stress. Combined gain- and loss-of-function evidence in mulberry establishes that *MuMYB116* functions as a key positive regulator of mulberry salt tolerance.

MuBPC2 positively regulates *MuMYB116* and enhances plant salt tolerance

To clarify the upstream regulatory cascade controlling *MuMYB116*, PlantTFDB analysis identified MuBPC2 as a potential binding partner of the *MuMYB116* promoter. Yeast one-hybrid analyses confirmed that MuBPC2 binds to the AATAGAGAGAGAAAGAGAGAGACT motif in the *MuMYB116* promoter, as evidenced by normal yeast growth on SD/-Leu + 200 ng·mL^{-1} AbA medium (Fig. 8a). To further verify this direct binding using purified proteins, we performed EMSA. Incubation of the biotin-labeled probe containing the target motif with GST-MuBPC2, but not GST alone, resulted in

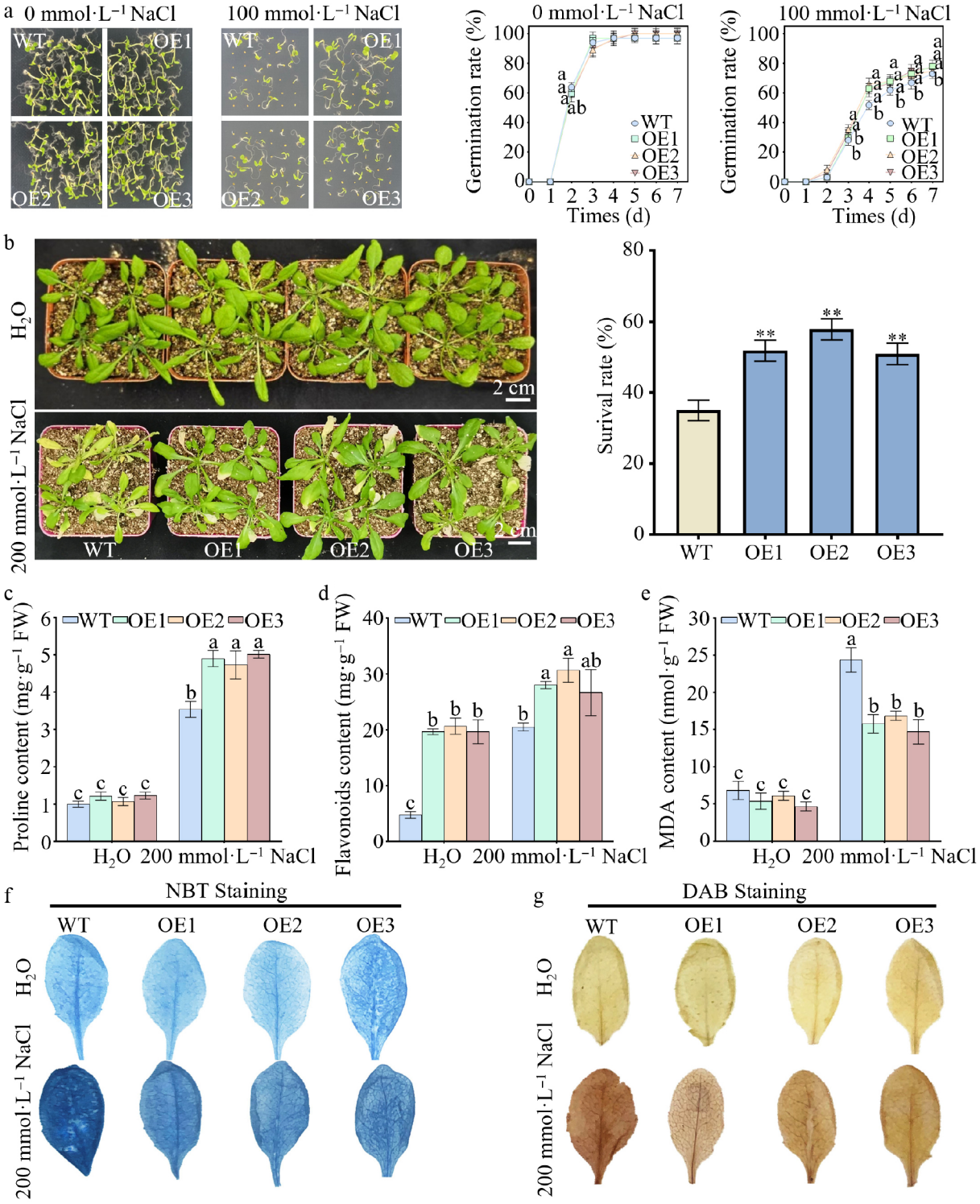


Fig. 4 Heterologous overexpression of *MuMYB116* enhances salt tolerance in transgenic *Arabidopsis*. (a) Germination kinetics of WT and *MuMYB116*-overexpressing (OE) seeds on 1/2 MS medium supplemented with 0 and 100 mmol·L^{-1} NaCl within 7 d. Data are presented as mean ± SD (n = 3 independent biological replicates; each replicate consisted of 100 individual seeds). Different lowercase letters indicate significant differences (one-way ANOVA with Tukey's HSD test, $p < 0.05$). (b) Phenotypes and survival rates of 4-week-old WT and OE plants after 200 mmol·L^{-1} NaCl stress. Data are presented as mean ± SD (n = 3 independent biological replicates; each replicate consisted of 50 individual plants); ** $p < 0.01$ (Student's t-test). Quantification of (c) proline, (d) total flavonoid, and (e) MDA content in WT and OE leaves under control and salt-stress conditions. Data are presented as mean ± SD (n = 3 biological replicates). Different lowercase letters indicate significant differences (one-way ANOVA with Tukey's HSD test, $p < 0.05$). Accumulation of O_2^- and H_2O_2 was visualized by (f) nitroblue tetrazolium (NBT) staining and (g) 3,3'-diaminobenzidine (DAB) staining.

a mobility-shifted band that was effectively outcompeted by an excess of unlabeled probe (Fig. 8b).

Dual-luciferase reporter assays showed that MuBPC2 significantly enhanced the transcriptional activity of the *MuMYB116* promoter

https://doi.org/10.48130/forres-0026-0035

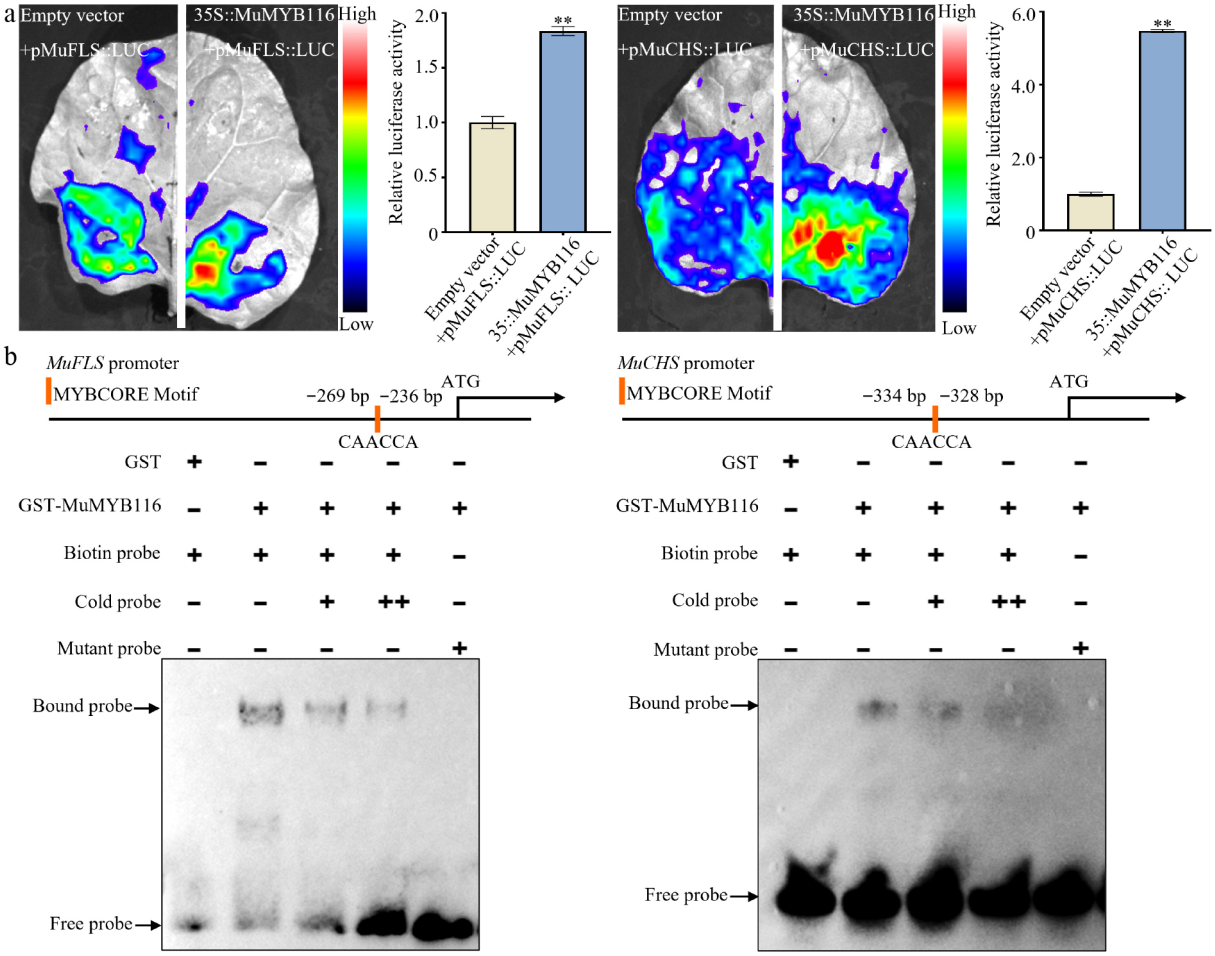


Fig. 5 MuMYB116 directly binds and activates the promoters of flavonoid biosynthetic genes *MuFLS* and *MuCHS*. (a) Dual-luciferase reporter assay showing transactivation of *MuFLS* and *MuCHS* promoters by MuMYB116. The effector plasmid (35S::MuMYB116) or empty vector (control) was co-infiltrated with reporter plasmids (pMuFLS::LUC or pMuCHS::LUC) into *Nicotiana benthamiana* leaves. LUC/REN ratios are shown. Data are presented as mean ± SD (n = 3 biological replicates). ** $p < 0.01$ (Student's t-test). (b) Electrophoretic mobility shift assay (EMSA) confirming direct binding of MuMYB116 to the MYBCORE motifs in the *MuFLS* and *MuCHS* promoters. Biotin-labeled probes containing the MYBCORE motifs were incubated with purified His-MuMYB116 protein or His alone (negative control). Unlabeled probes were used for competition assays. The shifted bands (indicated by arrows) indicate protein-DNA complexes.

(Fig. 8c). A GUS staining assay further confirmed elevated promoter activity of *MuMYB116* in the presence of MuBPC2 (Fig. 8d). In addition, semi-quantitative RT-PCR assays validated that MuBPC2 upregulated *MuMYB116* transcript abundance (Fig. 8e). These results collectively confirmed that MuBPC2 is a positive upstream regulator of *MuMYB116*.

qRT-PCR expression profiling further revealed that *MuBPC2* expression was markedly upregulated by exogenous ABA, MeJA, and NaCl, while GA treatment notably suppressed its expression (Fig. 9a). Importantly, the transcriptional profile of *MuBPC2* closely mirrored that of *MuMYB116*. This further supports the regulatory association between the two genes and implies their coordinated involvement in hormone signaling and salt-stress responses.

We next investigated the salt-tolerant function of MuBPC2 in mulberry through transient leaf disc overexpression. Under control conditions, no obvious difference was observed between the vector control and *MuBPC2*-overexpressing leaf discs. However, under 300 mmol·L^{-1} NaCl stress, leaf discs transiently overexpressing *MuBPC2* exhibited significantly enhanced salt tolerance (Fig. 9b) and higher chlorophyll content (Fig. 9c). Collectively, these observations suggest that transient *MuBPC2* overexpression in mulberry leaves effectively improved salt-stress tolerance.

Furthermore, salt-stress assays were performed on mulberry seedlings with *MuBPC2*-overexpressing hairy roots (OE). Under 300 mmol·L^{-1} NaCl treatment, seedlings carrying *MuBPC2*-overexpressing hairy roots showed significantly greater salt tolerance than the vector control, as evidenced by reduced leaf wilting and better growth (Fig. 9d). Statistical analysis further confirmed that overexpression of *MuBPC2* significantly increased the survival rate of mulberry seedlings upon salt-stress exposure (Fig. 9e). These data demonstrate that MuBPC2 enhances mulberry salt tolerance by activating *MuMYB116* transcription.

Interaction between MuMYB116 and MuCML44

Initial yeast two-hybrid library screening revealed that MuCML44, a calmodulin-like sensor protein, may physically associate with MuMYB116. To verify this interaction, a Y2H assay was performed. Yeast cells co-transformed with AD-MuMYB116 and BD-MuCML44 could grow normally on quadruple dropout (QDO) medium and produce blue coloration on QDO + X-α-gal medium (Fig. 10a). A

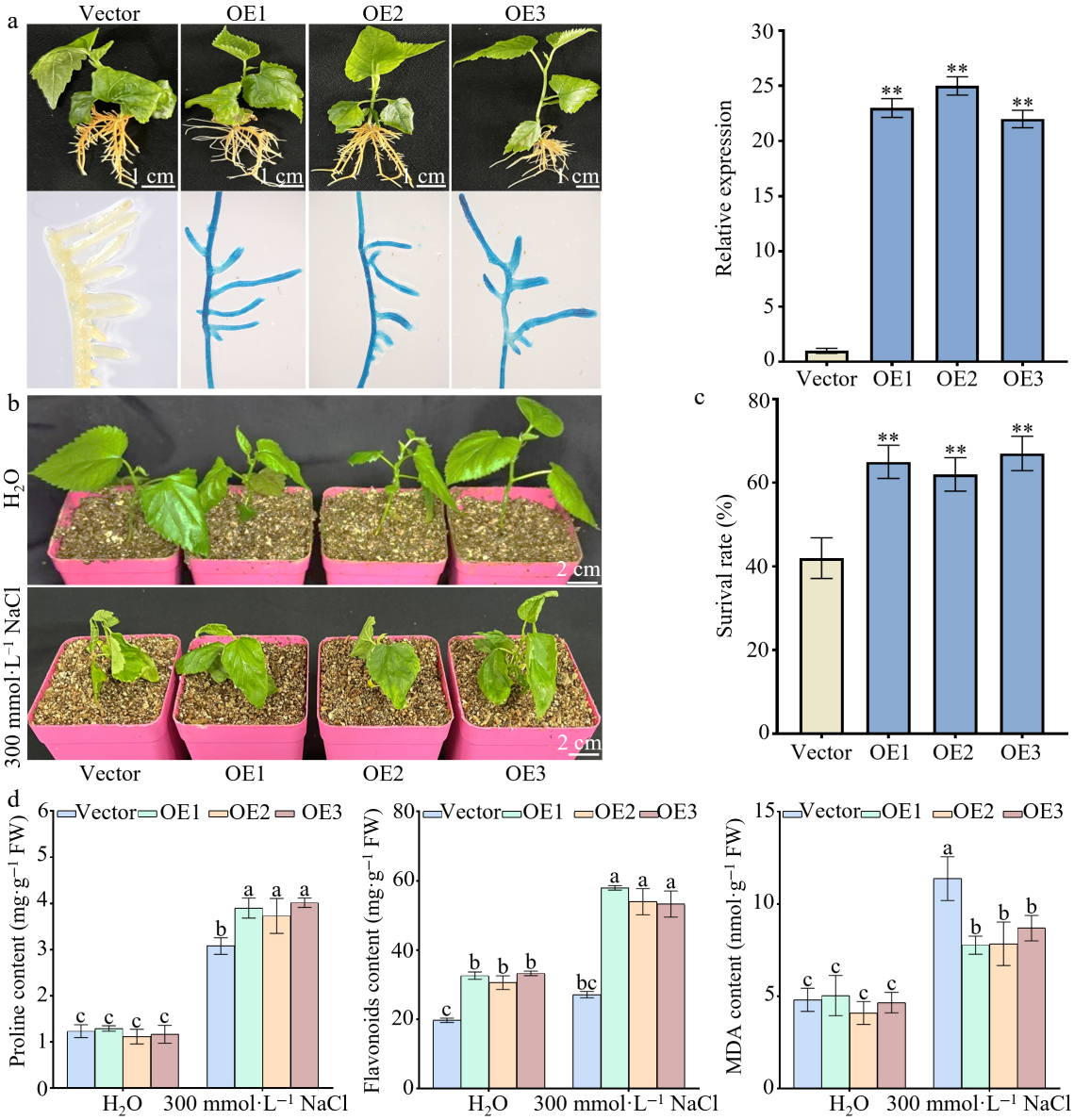


Fig. 6 Functional validation of *MuMYB116* in salt tolerance using mulberry hairy roots. (a) Identification of transgenic hairy roots and relative expression levels of *MuMYB116* in mulberry hairy roots transformed with an empty vector (Vector) or a *MuMYB116* overexpression construct (OE). GUS staining indicates that *MuMYB116* was successfully expressed in the hairy roots. Data are presented as mean ± SD (n = 3 biological replicates); ** $p < 0.01$ (Student's t-test). The scale bar value is 1 cm. (b) Phenotype of mulberry seedlings with transgenic hairy roots under 300 mmol·L^{-1} NaCl stress. (c) Survival rates of mulberry seedlings under 300 mmol·L^{-1} NaCl stress. Data are presented as mean ± SD (n = 3 independent biological replicates; each replicate consisted of 20 individual seedlings); ** $p < 0.01$ (Student's t-test). (d) Proline, flavonoid, and MDA content. Data are presented as mean ± SD (n = 3 biological replicates). Different lowercase letters indicate significant differences (one-way ANOVA with Tukey's HSD test, $p < 0.05$).

subsequent LCI assay in *N. benthamiana* leaves showed strong luminescence signals in tissues co-infiltrated with NLuc-MuMYB116 and CLuc-MuCML44, whereas no luminescence was detected in control groups (Fig. 10b). To further validate this interaction using purified proteins, we performed an *in vitro* pull-down assay. GST-MuMYB116, but not GST alone, was able to specifically pull down His-MuCML44, as detected using an anti-His antibody (Fig. 10c). This result confirms that MuMYB116 physically interacts with MuCML44.

MuCML44 functions as a canonical Ca^{2+} sensor protein that mediates abiotic-stress signal transduction in response to fluctuations in cytoplasmic Ca^{2+} levels[46]. The physical interaction between MuMYB116 and MuCML44 implied that MuMYB116-mediated salt tolerance may be associated with the calcium ion signaling pathway. To test this hypothesis, we pre-treated *MuMYB116*-OE and WT *Arabidopsis* seedlings with the Ca^{2+} channel inhibitor $LaCl_3$ prior to NaCl exposure. The results showed that $LaCl_3$ pretreatment significantly attenuated the salt tolerance of *MuMYB116*-OE *Arabidopsis*, as reflected by impaired growth (Fig. 10d) and reduced survival rates (Fig. 10e). However, growth remained better and survival rates remained higher in *MuMYB116*-OE seedlings treated with $LaCl_3$ than in WT seedlings, indicating that *MuMYB116* modulates salt tolerance through both Ca^{2+}-dependent and Ca^{2+}-independent regulatory pathways, suggesting the involvement of MuCML44-associated Ca^{2+} signaling.

https://doi.org/10.48130/forres-0026-0035

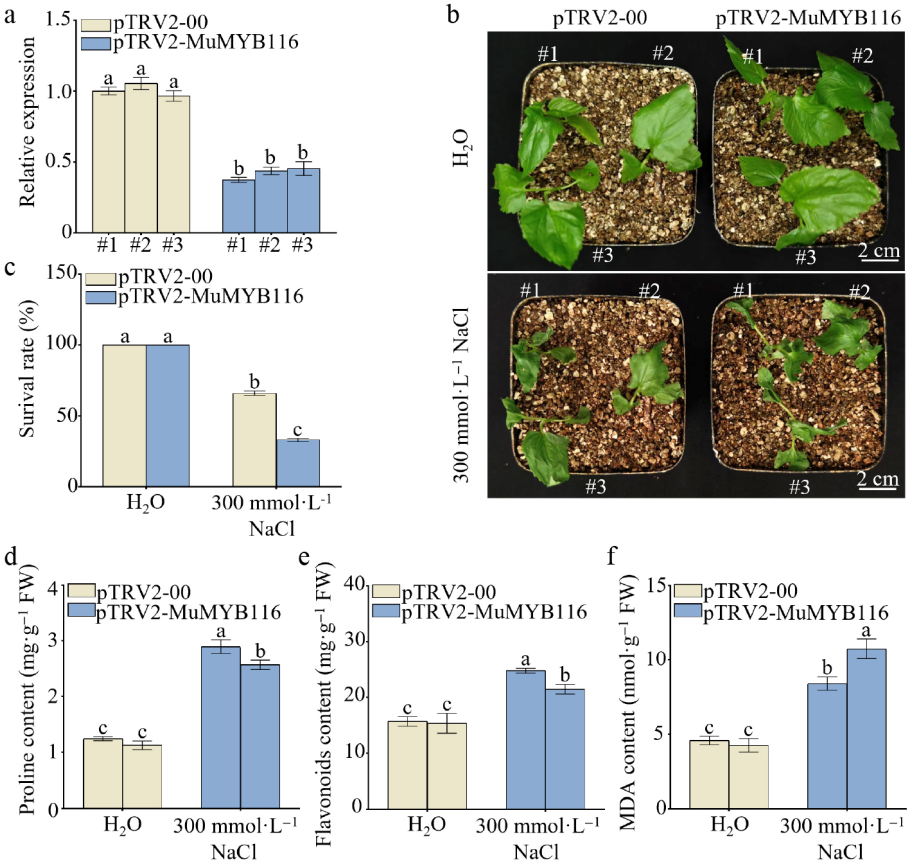


Fig. 7 VIGS-mediated silencing of *MuMYB116* impairs salt tolerance in mulberry. (a) qRT-PCR analysis confirming the silencing efficiency of *MuMYB116* in pTRV2-MuMYB116 seedlings compared with pTRV2-00 controls. Data are presented as mean ± SD (n = 3 biological replicates). (b) Phenotypes of pTRV2-00 (control) or pTRV2-MuMYB116 (silenced) mulberry seedlings under 0 or 300 mmol·L^{-1} NaCl stress for 7 d. (c) Survival rates of pTRV2-00 (control) or pTRV2-MuMYB116 (silenced) mulberry seedlings after 7 d of salt treatment. Data are presented as mean ± SD (n = 3 independent biological replicates; each replicate consisted of 20 individual seedlings). Physiological parameters of pTRV2-00 (control) or pTRV2-MuMYB116 (silenced) mulberry seedlings under salt stress: (d) proline, (e) flavonoid, and (f) MDA content. Data are presented as mean ± SD (n = 3 biological replicates). Different lowercase letters indicate significant differences (p < 0.05, one-way ANOVA with Tukey's HSD test).

Discussion

R2R3-MYB transcription factors coordinate plant abiotic stress adaptation by balancing defense responses and developmental homeostasis across diverse plant species[47–50]. However, their roles in mediating the growth-defense trade-off in woody perennials remain poorly understood. In this study, we functionally characterized *MuMYB116* and elucidated its function in orchestrating salt adaptation through a regulatory network integrating hormone signaling and Ca^{2+} transduction. Findings from both heterologous *Arabidopsis* and native mulberry systems consistently support a model in which *MuMYB116* serves as a central regulator of the balance between growth and defense, repressing development under favorable conditions and activating protective responses upon salt stress. This work provides high-value genetic resources for saline soil phytoremediation and molecular breeding of salt-tolerant mulberry.

MuMYB116 mediates the growth-defense trade-off

The growth-defense trade-off is an evolutionarily conserved adaptive strategy in plants, which optimizes the allocation of metabolic resources between growth and survival[51–53]. Our findings suggest that *MuMYB116* acts as an important regulator of this trade-off, balancing plant adaptability under fluctuating environmental conditions through context-dependent regulation.

Under non-stress conditions, *MuMYB116* moderately represses vegetative and reproductive growth, as evidenced by dwarfism, shortened primary roots, and delayed flowering in *MuMYB116*-overexpressing *Arabidopsis* (Fig. 3). Although these developmental phenotypes were characterized in a heterologous system, they imply a potentially conserved growth-regulatory function of MuMYB116 that may also be retained in mulberry. This growth repression may represent a resource conservation strategy, redirecting resources from growth toward the accumulation of carbohydrates, amino acid precursors, and secondary-metabolite intermediates. Consistent with this possibility, increased proline and flavonoid accumulation was observed in mulberry *MuMYB116*-overexpressing lines (Fig. 6d). This lays the foundation for the rapid activation of stress responses when plants are exposed to adverse conditions.

Under salt stress, *MuMYB116* shifts its regulatory activity toward enhanced stress resistance. Salinity stress and defense-related hormones (ABA, MeJA) induce *MuMYB116* expression (Fig. 2). In turn, *MuMYB116* activates a series of coordinated physiological mechanisms, including promoting the accumulation of the osmoprotectant proline, accelerating the accumulation of antioxidant flavonoids to scavenge ROS, and alleviating cell membrane oxidative damage (lower MDA content) (Figs. 4c–f, 6d). Notably, *MuFLS* and *MuCHS* are direct transcriptional targets of MuMYB116. However,

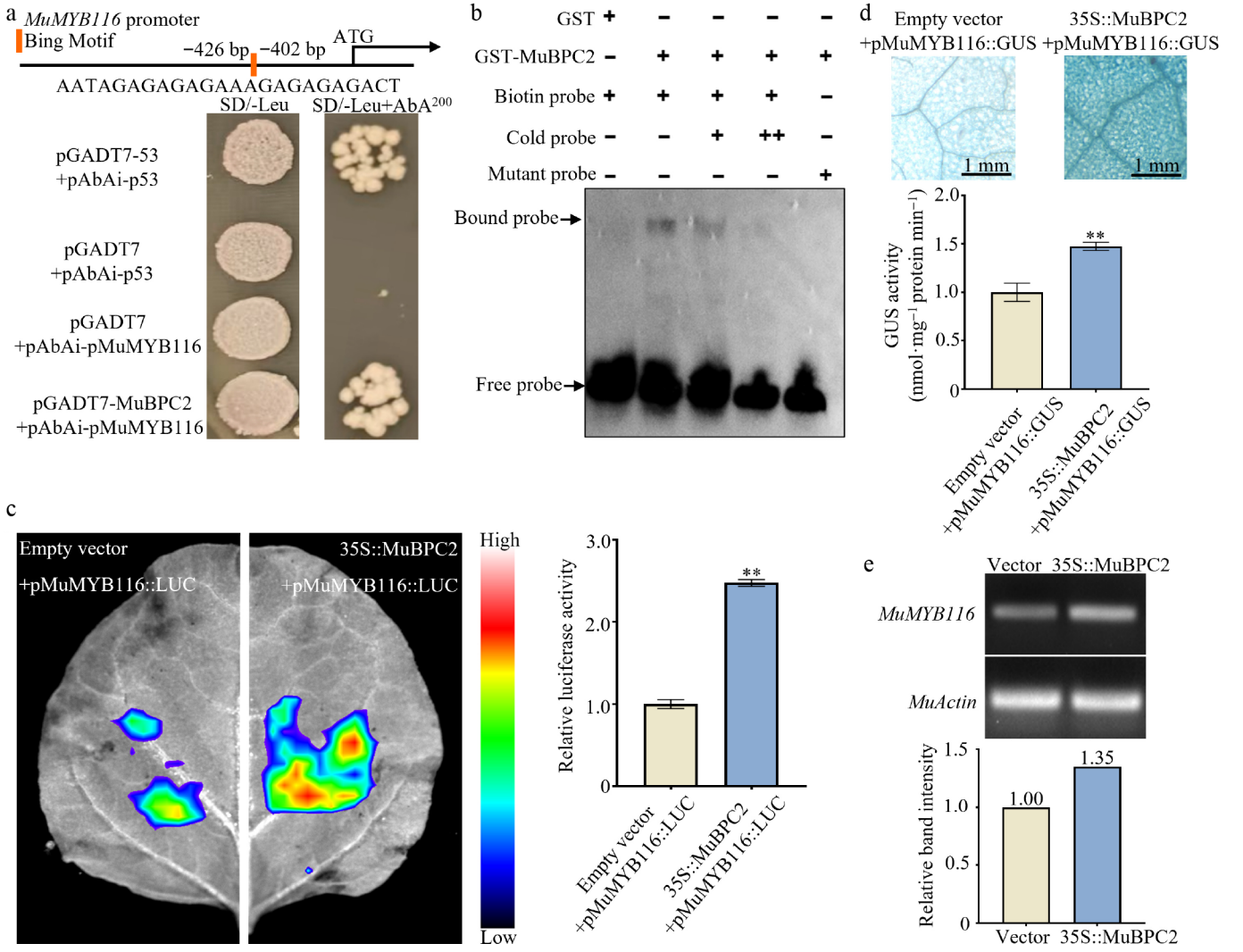


Fig. 8 MuBPC2 binds to the *MuMYB116* promoter and enhances its transcriptional activity. (a) Yeast one-hybrid (Y1H) assay verifying the binding of MuBPC2 to the *MuMYB116* promoter. Yeast strains carrying the pMuMYB116-bait and either the pGADT7-MuBPC2 or empty pGADT7 were grown on SD/-Leu medium with or without Aureobasidin A (AbA, 200 ng·mL^{-1}). (b) EMSA confirming the direct binding of MuBPC2 to the *MuMYB116* promoter. A biotin-labeled probe containing the MuBPC2-binding motif was incubated with GST-MuBPC2 fusion protein or GST alone (negative control). An unlabeled probe was used for competition assays. The shifted band (indicated by the arrow) indicates the protein–DNA complex. (c) Dual-luciferase reporter assay in *Nicotiana benthamiana* leaves. The effector plasmid (35S::MuBPC2) or empty vector (control) was co-infiltrated with the reporter plasmid (pMuMYB116::LUC). (d) GUS staining of *N. benthamiana* leaves co-infiltrated with the pMuMYB116::GUS reporter and either 35S::MuBPC2 or the vector control. (e) Semi-quantitative RT-PCR analysis showing the expression level of *MuMYB116* in mulberry leaf transiently overexpressing *MuBPC2* or empty vector (control). Data are presented as mean ± SD (n = 3 biological replicates); ** $p < 0.001$, (Student's t-test).

proline accumulation is interpreted as an indirect or synergistic downstream consequence, since we have not obtained target-binding evidence for the proline-biosynthetic gene *MuP5CS*. The direct transcriptional activation of flavonoid biosynthetic genes *MuFLS* and *MuCHS* by MuMYB116 provides a mechanistic basis for these physiological changes (Fig. 5).

Furthermore, the hormone-inducible expression profile of *MuMYB116* fine-tunes this growth-stress balance dynamically. Transcript levels of *MuMYB116* are elevated in response to salt stress, ABA, and MeJA, while GA treatment downregulates its expression (Fig. 2). This forms a hormone-mediated switch that enables rapid transcriptional reprogramming in response to environmental changes. This regulation prevents excessive growth inhibition under favorable conditions and ensures timely activation of stress responses. Such a dynamic regulatory mechanism is particularly advantageous for perennial mulberry plants subjected to long-term salt stress.

It is important to note that the growth-repressive phenotype under non-stress conditions was predominantly observed in the heterologous *Arabidopsis* system. While this suggests a conserved function of MuMYB116, the endogenous developmental regulation of MuMYB116 in mulberry, particularly its impact on vegetative and reproductive growth under optimal conditions, warrants further exploration. The primary focus of our mulberry experiments was on salt-stress responses, and long-term developmental phenotyping in the native host remains to be conducted.

Regulatory network and molecular mechanisms underlying *MuMYB116*-mediated salt tolerance

Based on the above results, we propose an integrated molecular model illustrating *MuMYB116*-mediated salt tolerance in mulberry (Fig. 11). MuMYB116 confers salt tolerance to mulberry,

https://doi.org/10.48130/forres-0026-0035

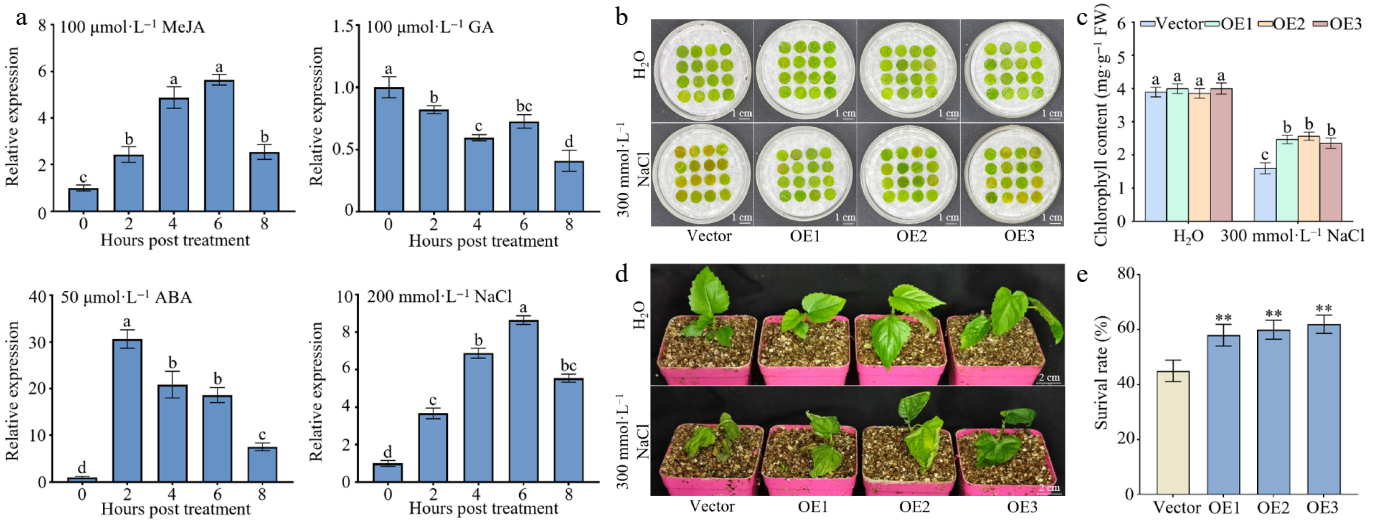


Fig. 9 Expression pattern and salt tolerance function of *MuBPC2* in mulberry. (a) qRT-PCR analysis of dynamic changes in *MuBPC2* transcription levels in mulberry seedlings in response to ABA, MeJA, GA, or NaCl treatments. Data are presented as mean ± SD (n = 3 biological replicates). Different lowercase letters indicate significant differences ($p < 0.05$, one-way ANOVA with Tukey's HSD test). (b) Phenotypes and (c) chlorophyll content of mulberry leaves transiently overexpressing *MuBPC2* incubated with 0 or 300 mmol·L^{-1} NaCl solution. Data are presented as mean ± SD (n = 3 independent biological replicates; each replicate consisted of 15 individual leaf discs). Different lowercase letters indicate significant differences ($p < 0.05$, one-way ANOVA with Tukey's HSD test). (d) Phenotypes and (e) survival rates of mulberry seedlings with transgenic empty vector (Vector) or *MuBPC2* (OE) hairy roots under 0 or 300 mmol·L^{-1} NaCl stress. Data are presented as mean ± SD (n = 3 independent biological replicates; each replicate consisted of 20 individual seedlings); ** $p < 0.01$ (Student's t-test).

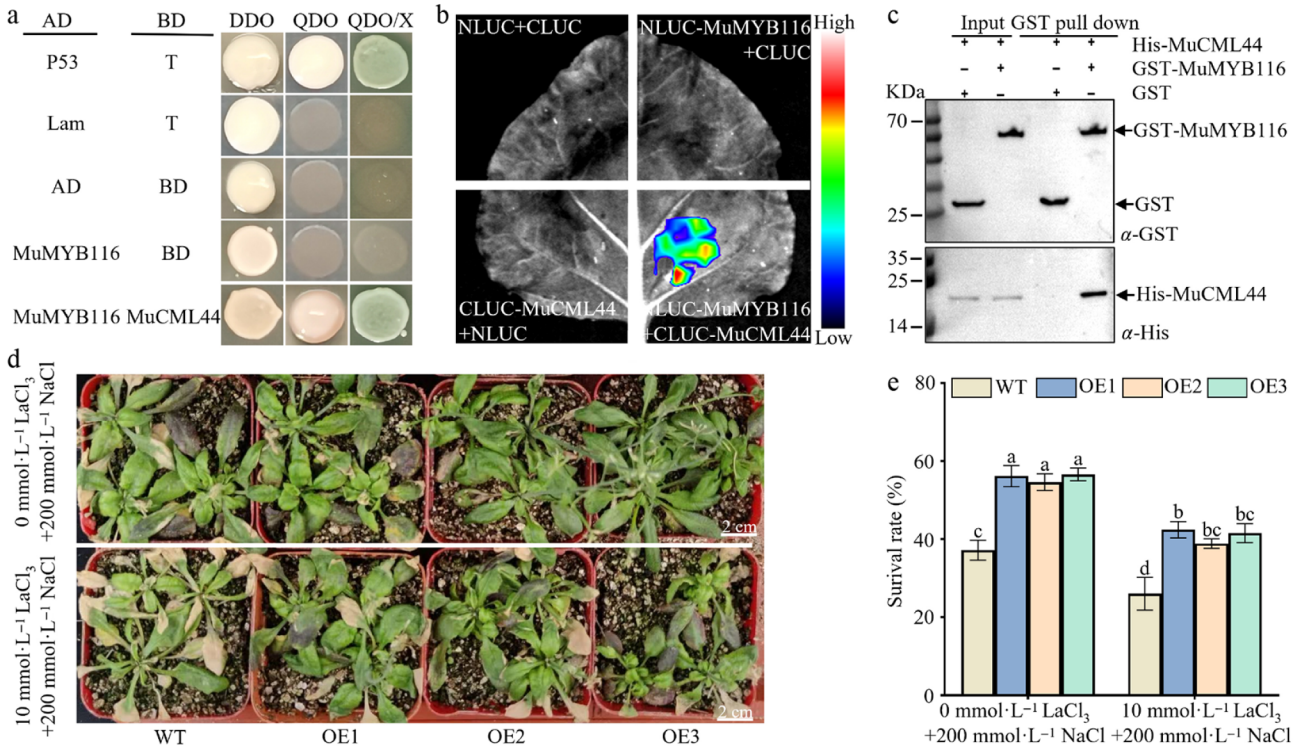


Fig. 10 Interaction between MuMYB116 and MuCML44 and involvement of Ca^{2+} signaling in MuMYB116-mediated salt tolerance. (a) Y2H assay confirming the interaction between MuMYB116 and MuCML44. Yeast cells co-transformed with BD-MuCML44 and AD-MuMYB116, or the indicated negative controls, were grown on synthetic dropout media: DDO (SD/-Trp/-Leu), QDO (SD/-Trp/-Leu/-Ade/-His), and QDO medium supplemented with X-α-gal. (b) LCI assay in *Nicotiana benthamiana* leaves. Strong luminescence indicates protein interaction. (c) *In vitro* pull-down assay confirming direct interaction between MuMYB116 and MuCML44. GST-MuMYB116 or GST alone was incubated with His-MuCML44. Bound proteins were analyzed by western blotting with anti-His (upper) and anti-GST (lower) antibodies. Input (10% of the total protein) is shown as a loading control. (d) Phenotypes of WT and *MuMYB116*-overexpressing (OE) *Arabidopsis* under 200 mmol·L^{-1} salt stress with or without 10 mmol·L^{-1} $LaCl_3$ (Ca^{2+} inhibitor) treatment. (e) Survival rate of WT and OE *Arabidopsis* under different treatments. Data are presented as mean ± SD (n = 3 independent biological replicates; each replicate consisted of 50 individual plants). Different lowercase letters indicate significant differences (one-way ANOVA with Tukey's HSD test, $p < 0.05$).

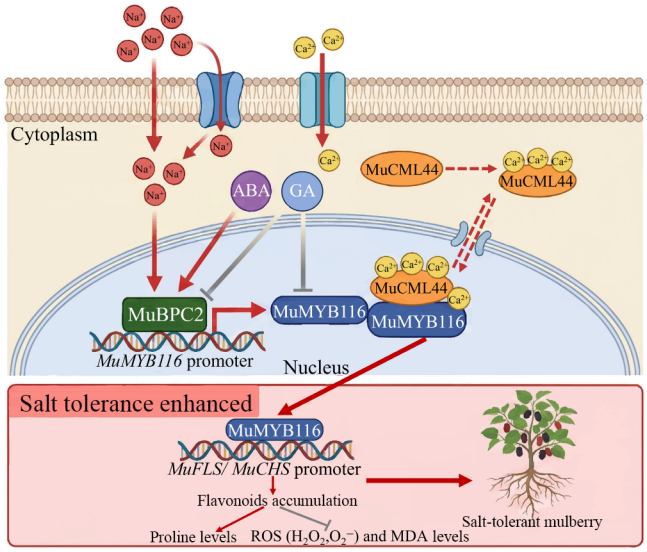


Fig. 11 Proposed working model of MuMYB116-mediated salt tolerance in mulberry. Salt stress induces *MuBPC2* expression through ABA/MeJA signaling. MuBPC2 binds the *MuMYB116* promoter and activates its transcription. Conversely, GA represses the transcription of both *MuBPC2* and *MuMYB116*. Meanwhile, MuCML44, a Ca^{2+}-binding protein, interacts with MuMYB116 and may link Ca^{2+} signaling to MuMYB116-mediated responses. The activated *MuMYB116* then promotes flavonoid and proline accumulation, enhances antioxidant capacity, and reduces ROS and MDA levels, ultimately improving salt tolerance.

encompassing upstream transcriptional regulation, downstream signal transduction, and hormone crosstalk. At the upstream regulatory level, stress-induced MuBPC2 functions as a crucial positive transcriptional activator of *MuMYB116*. MuBPC2 specifically binds to the *MuMYB116* promoter to enhance its transcriptional activity. Importantly, *MuBPC2* exhibits hormone- and salt-responsive expression patterns similar to those of *MuMYB116*. This implies that MuBPC2 may function as an upstream environmental signal sensor that responds to external stress and ABA signals, transmits these signals to *MuMYB116*, and amplifies the downstream stress-response cascade.

At the intermediate signaling level, MuMYB116 contributes to salt tolerance primarily through its association with MuCML44 and Ca^{2+} signaling. As a calmodulin-like protein, MuCML44 serves as a Ca^{2+} sensor that detects stress-elicited fluctuations in cytoplasmic Ca^{2+} concentration, which constitute an important early signal in plant salt-stress responses[54–56]. The physical interaction between MuMYB116 and MuCML44 establishes a critical molecular bridge linking cytoplasmic Ca^{2+} signal perception to nuclear transcriptional regulation. The current evidence supports their physical interaction and involvement in Ca^{2+} signaling; however, the detailed regulatory mechanism and the nature of the MuCML44–Ca^{2+} signaling cascade require further investigation. $LaCl_3$ treatment impairs *MuMYB116*-mediated salt tolerance, yet residual salt tolerance remains detectable. This suggests that *MuMYB116* may regulate salt-stress responses through both Ca^{2+}-dependent (MuCML44-mediated) and Ca^{2+}-independent signaling branches.

At the downstream functional layer, MuMYB116 directly targets the flavonoid biosynthetic genes *MuFLS* and *MuCHS* by binding to MYBCORE motifs in their promoters, facilitating flavonoid accumulation. Although proline accumulation was observed in *MuMYB116*-overexpressing lines, *MuP5CS* was not verified as a direct target of MuMYB116. Therefore, proline accumulation is likely induced by indirect or synergistic regulatory pathways. Flavonoids act as major nonenzymatic cellular antioxidants that scavenge excess ROS, explaining the reduced MDA and alleviated leaf injury observed in *MuMYB116*-overexpressing lines. This direct transcriptional activation of antioxidant metabolic genes eliminates the possibility that elevated flavonoid levels are merely secondary consequences of stress. This observation underscores the robustness and redundancy of plant stress-response networks, which ensure adaptive capacity in response to complex environmental cues.

Moreover, MuMYB116 acts as a core hub integrating multiple hormone signals to modulate salt tolerance. The shared hormone response patterns of *MuBPC2* and *MuMYB116* support a linear regulatory cascade that precisely modulates MuMYB116 activity in response to environmental changes, providing a molecular framework for plants to continuously optimize the growth-defense trade-off under fluctuating salinity conditions.

Conclusions

In summary, our multi-system functional characterization establishes MuMYB116 as a key regulatory node coordinating growth and salt-stress responses in mulberry. It suppresses development under favorable conditions while activating protective mechanisms upon salt exposure. *MuMYB116* is transcriptionally activated by upstream MuBPC2 and physically interacts with MuCML44, linking MuMYB116 to Ca^{2+} signaling. Furthermore, MuMYB116 directly activates the flavonoid biosynthetic genes *MuFLS* and *MuCHS* to enhance antioxidant capacity. Collectively, MuMYB116 mediates a hormone-regulated growth-defense trade-off. These findings offer novel insights into the molecular mechanisms underpinning salt tolerance in woody plants and provide genetic resources for breeding salt-tolerant mulberry cultivars, supporting sustainable mulberry cultivation and ecological restoration of saline soils worldwide.

Author contributions

The authors confirm their contributions to the paper as follows: conceptualization, writing – review and editing, supervision and funding acquisition: Ji X, Gai Y; methodology: Liu C, Zhao T, Sun M; validation: Lu S, Yv L; formal analysis, writing – original draft preparation: Liu C, Zhao T; investigation: Liu C, Zhao T, Sun M, Wang G; visualization: Liu Z; project administration: Ji X. All authors reviewed the results and approved the final version of the manuscript.

Data availability

All data that underpin the conclusions drawn in this work can be found in the main text as well as the supplementary files accompanying this article.

Acknowledgments

This study received funding from the National Natural Science Foundation of China (Grant Nos 32171748 and 32172799), the Natural Science Foundation of Shandong Province (Grant Nos ZR2024MC211 and ZR2025QC308), and the Modern Agricultural Technology System of Shandong Province (Grant No. SDAIT-18-04).

Conflict of interest

The authors declare that they have no conflict of interest.

Supplementary information accompanies this paper online at: https://doi.org/10.48130/forres-0026-0035.

Dates

Received 27 February 2026; Revised 26 August 2026; Accepted 16 October 2026; Published online 9 November 2026

References

[1] Xu N, Wang T, Wang Y, Dong J, Shaopeng Y. 2025. Coordinated roles of osmotic adjustment, antioxidant defense, and ion homeostasis in the salt tolerance of mulberry (*Morus alba* L.'Tailai Sang') seedlings. *Forests* 16:1258

[2] Kaushal R, Kumar A, Mandal D, Tomar JMS, Jinger D, et al. 2024. Mulberry based agroforestry system and canopy management practices to combat soil erosion and enhancing carbon sequestration in degraded lands of Himalayan foothills. *Environmental and Sustainability Indicators* 24:100467

[3] Maqsood M, Anam Saeed R, Sahar A, Khan MI. 2022. Mulberry plant as a source of functional food with therapeutic and nutritional applications: a review. *Journal of Food Biochemistry* 46:e14263

[4] Jia Z, Tang M, Wu J. 1999. The determination of flavonoid contents in mulberry and their scavenging effects on superoxide radicals. *Food Chemistry* 64:555–559

[5] Du Q, Zheng J, Xu Y. 2008. Composition of anthocyanins in mulberry and their antioxidant activity. *Journal of Food Composition and Analysis* 21:390–395

[6] Sun Z, Yin Y, Zhu W, Zhou Y. 2023. Morphological, physiological, and biochemical composition of mulberry (*Morus* spp.) under drought stress. *Forests* 14:949

[7] Guha A, Sengupta D, Kumar Rasineni G, Ramachandra Reddy A. 2010. An integrated diagnostic approach to understand drought tolerance in mulberry (*Morus indica* L.). *Flora - Morphology, Distribution, Functional Ecology of Plants* 205:144–151

[8] Baciu ED, Baci GM, Moise AR, Dezmirean DS. 2023. A status review on the importance of mulberry (*Morus* spp.) and prospects towards its cultivation in a controlled environment. *Horticulturae* 9:444

[9] Acharya R, Ahmad SR, Gangopadhyay D, Shaw S, Manna A, et al. 2026. Mulberry-based bio-reclamation of salinity-degraded landscapes. *iScience* 29:116566

[10] Qadir M, Ghafoor A, Murtaza G. 2000. Amelioration strategies for saline soils: a review. *Land Degradation & Development* 11:501–521

[11] Corwin DL. 2021. Climate change impacts on soil salinity in agricultural areas. *European Journal of Soil Science* 72:842–862

[12] Yang Y, Guo Y. 2018. Elucidating the molecular mechanisms mediating plant salt-stress responses. *New Phytologist* 217:523–539

[13] Acosta-Motos J, Ortuño M, Bernal-Vicente A, Diaz-Vivancos P, Sanchez-Blanco M, et al. 2017. Plant responses to salt stress: adaptive mechanisms. *Agronomy* 7:18

[14] Munns R, Tester M. 2008. Mechanisms of salinity tolerance. *Annual Review of Plant Biology* 59:651–681

[15] Lu N, Luo Z, Ke Y, Dai L, Duan H, et al. 2017. Growth, physiological, biochemical, and ionic responses of *Morus alba* L. seedlings to various salinity levels. *Forests* 8:488

[16] Vijayan K, Chakraborti SP, Ercisli S, Ghosh PD. 2008. NaCl induced morpho-biochemical and anatomical changes in mulberry (*Morus* spp.). *Plant Growth Regulation* 56:61–69

[17] Agastian P, Kingsley SJ, Vivekanandan M. 2000. Effect of salinity on photosynthesis and biochemical characteristics in mulberry genotypes. *Photosynthetica* 38:287–290

[18] Ramachandra Reddy A, Chaitanya KV, Jutur PP, Sumithra K. 2004. Differential antioxidative responses to water stress among five mulberry (*Morus alba* L.) cultivars. *Environmental and Experimental Botany* 52:33–42

[19] Singh KB, Foley RC, Oñate-Sánchez L. 2002. Transcription factors in plant defense and stress responses. *Current Opinion in Plant Biology* 5:430–436

[20] Hoang XLT, Nhi DNH, Thu NBA, Thao NP, Tran LP. 2017. Transcription factors and their roles in signal transduction in plants under abiotic stresses. *Current Genomics* 18:483–497

[21] Song L, Huang SC, Wise A, Castanon R, Nery JR, et al. 2016. A transcription factor hierarchy defines an environmental stress response network. *Science* 354:aag1550

[22] Chen WJ, Zhu T. 2004. Networks of transcription factors with roles in environmental stress response. *Trends in Plant Science* 9:591–596

[23] Kidokoro S, Shinozaki K, Yamaguchi-Shinozaki K. 2022. Transcriptional regulatory network of plant cold-stress responses. *Trends in Plant Science* 27:922–935

[24] Martin C, Paz-Ares J. 1997. MYB transcription factors in plants. *Trends in Genetics* 13:67–73

[25] Dubos C, Stracke R, Grotewold E, Weisshaar B, Martin C, et al. 2010. MYB transcription factors in *Arabidopsis*. *Trends in Plant Science* 15:573–581

[26] Liu J, Osbourn A, Ma P. 2015. MYB transcription factors as regulators of phenylpropanoid metabolism in plants. *Molecular Plant* 8:689–708

[27] Wu Y, Wen J, Xia Y, Zhang L, Du H. 2022. Evolution and functional diversification of R2R3-MYB transcription factors in plants. *Horticulture Research* 9:uhac058

[28] Feng G, Burleigh JG, Braun EL, Mei W, Barbazuk WB. 2017. Evolution of the 3R-MYB gene family in plants. *Genome Biology and Evolution* 9:1013–1029

[29] Du H, Wang YB, Xie Y, Liang Z, Jiang SJ, et al. 2013. Genome-wide identification and evolutionary and expression analyses of MYB-related genes in land plants. *DNA Research* 20:437–448

[30] Cao Y, Li K, Li Y, Zhao X, Wang L. 2020. MYB transcription factors as regulators of secondary metabolism in plants. *Biology* 9:61

[31] Dai X, Xu Y, Ma Q, Xu W, Wang T, et al. 2007. Overexpression of an R1R2R3 MYB gene, *OsMYB3R - 2*, increases tolerance to freezing, drought, and salt stress in transgenic Arabidopsis. *Plant Physiology* 143:1739–1751

[32] Zhang P, Wang R, Yang X, Ju Q, Li W, et al. 2020. The R2R3-MYB transcription factor AtMYB49 modulates salt tolerance in *Arabidopsis* by modulating the cuticle formation and antioxidant defence. *Plant, Cell & Environment* 43:1925–1943

[33] Song Y, Tang H, Zhang Z, Sun X, Ding X, et al. 2025. A novel MsEOBI-*MsPAL1* module enhances salinity stress tolerance, floral scent emission and seed yield in alfalfa. *Plant, Cell & Environment* 48:907–922

[34] Xu R, Wang Y, Zheng H, Lu W, Wu C, et al. 2015. Salt-induced transcription factor *MYB74* is regulated by the RNA-directed DNA methylation pathway in *Arabidopsis*. *Journal of Experimental Botany* 66:5997–6008

[35] Li B, Fan R, Guo S, Wang P, Zhu X, et al. 2019. The Arabidopsis MYB transcription factor, MYB111 modulates salt responses by regulating flavonoid biosynthesis. *Environmental and Experimental Botany* 166:103807

[36] Du B, Liu H, Dong K, Wang Y, Zhang Y. 2022. Over-expression of an R2R3 MYB gene, *MdMYB108L*, enhances tolerance to salt stress in transgenic plants. *International Journal of Molecular Sciences* 23:9428

[37] Cui F, Brosché M, Sipari N, Tang S, Overmyer K. 2013. Regulation of ABA dependent wound induced spreading cell death by MYB108. *New Phytologist* 200:634–640

[38] Du SX, Wang LL, Yu WP, Xu SX, Chen L, et al. 2024. Appropriate induction of TOC1 ensures optimal MYB44 expression in ABA signaling and stress response in *Arabidopsis*. *Plant, Cell & Environment* 47:3046–3062

[39] Yan C, Chai J, Zheng Q, Li S, Li M, et al. 2026. The MYB transcription factors directly mediate abscisic acid signals in response to abiotic stress. *Plant Science* 363:112890

[40] Li T, Qi X, Zeng Q, Xiang Z, He N. 2014. MorusDB: a resource for mulberry genomics and genome biology. *Database* 2014:bau054

[41] Livak KJ, Schmittgen TD. 2001. Analysis of relative gene expression data using real-time quantitative PCR and the $2^{-\Delta\Delta CT}$ method. *Methods* 25:402–408

[42] Wang HR, Han SM, Wang DH, Zhao ZR, Ling H, et al. 2024. Unraveling the contribution of *MuISOS2* in conferring salinity tolerance in mulberry (*Morus atropurpurea* Roxb). *International Journal of Molecular Sciences* 25:3628

[43] Tripathi JM, Khan BR, Gaur R, Yadav D, Verma KK, et al. 2025. Gibberellic acid improves photosynthetic electron transport and stomatal function in crops that are adversely affected by salinity exposure. *Plants* 14:3388

[44] Shraim AM, Ahmed TA, Rahman MM, Hijji YM. 2021. Determination of total flavonoid content by aluminum chloride assay: a critical evaluation. *LWT* 150:111932

[45] Laval-Martin DL. 1985. Spectrophotometric method of controlled pheophytinization for the determination of both chlorophylls and pheophytins in plant extracts. *Analytical Biochemistry* 149:121–129

[46] Munir S, Liu H, Xing Y, Hussain S, Ouyang B, et al. 2016. Overexpression of calmodulin-like (*ShCML44*) stress-responsive gene from *Solanum habrochaites* enhances tolerance to multiple abiotic stresses. *Scientific Reports* 6:31772

[47] Soler M, Camargo ELO, Carocha V, Cassan-Wang H, San Clemente H, et al. 2015. The *E ucalyptus grandis* R2R3- MYB transcription factor family: evidence for woody growth-related evolution and function. *New Phytologist* 206:1364–1377

[48] Zhang J, Xie M, Tuskan GA, Muchero W, Chen JG. 2018. Recent advances in the transcriptional regulation of secondary cell wall biosynthesis in the woody plants. *Frontiers in Plant Science* 9:1535

[49] Guo H, Wang Y, Wang L, Hu P, Wang Y, et al. 2017. Expression of the MYB transcription factor gene *BplMYB46* affects abiotic stress tolerance and secondary cell wall deposition in *Betula platyphylla*. *Plant Biotechnology Journal* 15:107–121

[50] Han X, Zhao Y, Chen Y, Xu J, Jiang C, et al. 2022. Lignin biosynthesis and accumulation in response to abiotic stresses in woody plants. *Forestry Research* 2:9

[51] He Z, Webster S, He SY. 2022. Growth–defense trade-offs in plants. *Current Biology* 32:R634–R639

[52] Huot B, Yao J, Montgomery BL, He SY. 2014. Growth–defense tradeoffs in plants: a balancing act to optimize fitness. *Molecular Plant* 7:1267–1287

[53] Hou M, Xu G. 2025. Growth-defense trade-off in plants: from hypothesis to principle to paradigm. *Cell Host & Microbe* 33:1222–1226

[54] Zhu X, Perez M, Aldon D, Galaud JP. 2017. Respective contribution of CML8 and CML9, two *Arabidopsis* calmodulin-like proteins, to plant stress responses. *Plant Signaling & Behavior* 12:e1322246

[55] Bisht D, Mishra S, Bihani SC, Seth T, Srivastava AK, et al. 2025. Salt stress tolerance and calcium signalling components: where we stand and how far we can go? *Journal of Plant Growth Regulation* 44:1429–1447

[56] Hau B, Symonds K, Teresinski H, Janssen A, Duff L, et al. 2024. *Arabidopsis* calmodulin-like proteins CML13 and CML14 interact with calmodulin-binding transcriptional activators and function in salinity stress response. *Plant & Cell Physiology* 65:282–300

Copyright: © 2026 by the author(s). Published by Maximum Academic Press, Fayetteville, GA. This article is an open access article distributed under Creative Commons Attribution License (CC BY 4.0), visit https://creativecommons.org/licenses/by/4.0/.